SUPPLEMENTARY INFORMATION

SUPPLEMENTARY REFERENCES

Baba T, Ara T, Hasegawa M, Takai Y, Okumura Y, Baba M, Datsenko KA, Tomita M, Wanner BL, Mori H (2006) Construction of Escherichia coli K-12 in-frame, single-gene knockout mutants: the Keio collection. *Mol Syst Biol* **2:** 2006 0008

Desvaux M, Scott-Tucker A, Turner SM, Cooper LM, Huber D, Nataro JP, Henderson IR (2007) A conserved extended signal peptide region directs posttranslational protein translocation via a novel mechanism. *Microbiology* **153**(Pt 1)**:** 59-70

Dieterle F, Ross A, Schlotterbeck G, Senn H (2006) Probabilistic quotient normalization as robust method to account for dilution of complex biological mixtures. Application in 1H NMR metabonomics. *Anal Chem* **78**(13)**:** 4281-4290

Knowles TJ, Sridhar P, Rajesh S, Manoli E, Overduin M, Henderson IR (2010) Secondary structure and (1)H, (13)C and (15)N resonance assignments of BamE, a component of the outer membrane protein assembly machinery in Escherichia coli. *Biomol NMR Assign*

Laskowski RA, MacArthur MW, Moss DS, Thornton JM (1993) PROCHECK: a program to check the stereochemical quality of protein structures. *Journal of Applied Crystallography* **26**(2)**:** 283-291

Linge JP, O'Donoghue SI, Nilges M (2001) Automated assignment of ambiguous nuclear overhauser effects with ARIA. *Methods Enzymol* **339:** 71-90

Parsons HM, Ludwig C, Günther UL, Viant MR (2007) Improved classification accuracy in 1- and 2-dimensional NMR metabolomics data using the variance stabilising generalised logarithm transformation. *BMC Bioinformatics* **8:** 234

Southam AD, Payne TG, Cooper HJ, Arvanitis TN, Viant MR (2007) Dynamic Range and Mass Accuracy of Wide-Scan Direct Infusion Nanoelectrospray Fourier Transform Ion Cyclotron Resonance Mass Spectrometry-Based Metabolomics Increased by the Spectral Stitching Method. *Anal Chem* **79**(12)**:** 4595-4602

Tan CA, Roberts MF (1996) Vanadate is a potent competitive inhibitor of phospholipase C from Bacillus cereus. *Biochim Biophys Acta* **1298**(1)**:** 58-68

Wu H, Southam AD, Hines A, Viant MR (2008) High throughput tissue extraction protocol for NMR- and MS-based metabolomics. *Anal Biochem* **372**(2)**:** 204-212

Table S1. Structural statistics of the ensemble of 20 BamE solution structures

Parameter	*Value*
Number of restraints	
NOE	
Total	890
Intraresidue ($i = j$)	180
Sequential ($\|i - j\| = 1$)	274
Medium range ($1 < \|i - j\| \leq 4$)	161
Long range ($\|i - j\| > 4$)	275
Hydrogen bond restraints	15
Dihedral angle restraints	125
Rms deviation from distance restraints[a] (Å)	0.020 ± 0.002
Rms deviation from covalent geometry[a]	
Bond lengths (Å)	0.004 ± 0.000
Angles (deg.)	0.456 ± 0.020
Impropers (deg.)	1.383 ± 0.109
Ramachandran plot[b] (%)	
most favoured regions	74.8%
additionally allowed regions	20.9%
generously allowed regions	2.2%
disallowed regions	2.1%
RMSD (Å)	
Backbone (40-108)	1.51
Backbone (Absent flexible loops – 62-69 & 77-88)	0.83
Heavy atoms (40-108)	2.18
Heavy atoms (Absent flexible loops – 62-69 & 77-88)	1.42

[a] Evaluated by ARIA1.2 (Linge et al, 2001)

[b] Calculated for residues Ala21-Ser174 with PROCHECK-NMR (Laskowski et al, 1993)

Table S2: Abundance of the identified PE and PG species in wild type (WT) and two independent BamE Knockouts derived from KEIO Collection (M1 and M2). The results show the phosphatidylethanolamine (PE, highlighted in green) and phosphatidylglycerol (PG, highlighted in orange) species identified in the *E. coli* outer membrane samples, including the measured and theoretical *m/z* values and corresponding mass error, the statistical significance (ANOVA with Benjamini and Hochberg correction for multiple hypothesis testing), and the fold changes between the wild type and mutants. A group of shorter-chain, saturated PE species show small but significant differences between wild type and mutants (highlighted in blue), which may merit further studies.

m/z value	*p* value	WT/M1	WT/M2	Av. signal intensity	Putative lipid ID	theoretical *m/z*	mass error (Da)
606.41449	0.012	1.80	1.54	3644	PE 26:0	606.41403	7.61E-07
620.43059	0.022	1.78	1.32	14531	PE 27:0	620.42968	1.47E-06
632.43100	0.038	1.55	1.32	1989	PE 28:1	632.42968	2.09E-06
634.44647	0.025	1.83	1.41	91181	PE 28:0	634.44533	1.80E-06
637.40949	0.124	1.36	1.40	9733	PG 26:0	637.40861	1.38E-06
646.44650	0.159	1.48	1.26	14360	PE 29:1	646.44533	1.81E-06
648.46202	0.032	2.33	1.29	219850	PE 29:0	648.46098	1.61E-06
651.42554	0.073	1.58	1.29	23732	PG 27:0	651.42426	1.97E-06
660.46230	0.214	1.33	1.11	59400	PE 30:1	660.46098	2.00E-06
662.47610	0.079	1.70	1.15	1959127	PE 30:0	662.47663	-7.99E-07
663.42320	0.182	1.49	1.08	4265	PG 28:1	663.42426	-1.60E-06
665.44120	0.160	1.41	1.48	138997	PG 28:0	665.43991	1.94E-06
674.47728	0.214	1.54	1.06	480432	PE 31:1	674.47663	9.65E-07
676.49194	0.073	1.77	1.04	1477680	PE 31:0	676.49228	-5.01E-07
677.44134	0.306	1.28	1.10	19330	PG 29:1	677.43991	2.11E-06
679.45645	0.189	1.72	1.28	465666	PG 29:0	679.45556	1.31E-06
686.47787	0.911	0.99	0.95	3787	PE 32:2	686.47663	1.81E-06
688.49164	0.160	1.31	0.88	1781291	PE 32:1	688.49228	-9.28E-07
690.50742	0.153	1.63	1.12	1654371	PE 32:0	690.50793	-7.38E-07
691.45731	0.759	1.07	0.94	113682	PG 30:1	691.45556	2.53E-06
693.47048	0.278	1.37	1.05	3065855	PG 30:0	693.47121	-1.05E-06
700.49365	0.778	1.08	1.02	36921	PE 33:2	700.49228	1.96E-06
702.50592	0.306	1.22	0.94	8740499	PE 33:1	702.50793	-2.86E-06
705.47208	0.935	0.99	0.94	668132	PG 31:1	705.47121	1.23E-06
707.48610	0.257	1.37	1.00	3299421	PG 31:0	707.48686	-1.07E-06
714.50902	0.306	1.17	0.82	240103	PE 34:2	714.50793	1.53E-06
716.52390	0.264	1.15	0.83	1469925	PE 34:1	716.52358	4.47E-07
719.48594	0.306	1.05	0.81	3429975	PG 32:1	719.48686	-1.28E-06
721.50060	0.499	1.28	1.06	5277276	PG 32:0	721.50251	-2.65E-06
728.52527	0.073	0.69	1.07	113766	PE 35:2	728.52358	2.32E-06
730.53891	0.216	1.26	0.89	2142098	PE 35:1	730.53923	-4.37E-07
731.48767	0.357	0.95	0.83	29963	PG 33:2	731.48686	1.11E-06
733.50009	0.564	0.96	0.83	10585334	PG 33:1	733.50251	-3.30E-06
742.54032	0.079	1.53	0.71	767195	PE 36:2	742.53923	1.47E-06
744.55698	0.124	1.29	0.71	84634	PE 36:1	744.55488	2.82E-06
745.50385	0.214	0.84	0.62	241666	PG 34:2	745.50251	1.80E-06
747.51758	0.306	0.84	0.70	2387631	PG 34:1	747.51816	-7.75E-07
756.55658	0.781	0.89	0.92	55878	PE 37:2	756.55488	2.25E-06
759.51918	0.073	0.51	0.75	135987	PG 35:2	759.51816	1.34E-06
761.53280	0.348	0.99	0.73	3593680	PG 35:1	761.53381	-1.33E-06
770.57230	0.038	1.69	0.68	84308	PE 38:2	770.57053	2.30E-06
773.53472	0.159	0.96	0.54	695755	PG 36:2	773.53381	1.18E-06
775.55082	0.216	0.98	0.48	227110	PG 36:1	775.54946	1.75E-06
787.55121	0.306	0.68	0.73	94077	PG 37:2	787.54946	2.22E-06
801.56670	0.132	1.49	0.49	141537	PG 38:2	801.56511	1.98E-06

Table S3. Oligonucleotide primers used in this study.

[a] K= G or T, M= C or A

Name	Sequence[a]
T7 Promoter	5'-TAATACGACTCACTATAGGG-3’
T7 Terminator	5'-GCTAGTTATTGCTCAGCGG-3’
BamE NdeI	5'-CTGCTCGTACATATGCGCTGTAAAACGCTGAC-3’
BamE EcoRI	5'-CCGGAATTCTTAGTTACCACTCAGCGC-3’
BamE 20	5'-GATGTTGACCGCAGGCGGCTCCACTCTGGAGCGAG-3’
BamE 21	5'-GTTGACCGCAGGCTGTKGCACTCTGGAGCGAGTG-3’
BamE 22	5'-GACCGCAGGCTGTTCCKGCCTGGAGCGAGTGGTTTAC-3’
BamE 23	5'-GCAGGCTGTTCCACTKGCGAGCGAGTGGTTTAC-3’
BamE 24	5'-GGCTGTTCCACTCTGKGCCGAGTGGTTTACCGTC-3’
BamE 25	5'-CTGTTCCACTCTGGAGKGCGTGGTTTACCGTCCTG-3’
BamE 26	5'-GTTCCACTCTGGAGCGAKGCGTTTACCGTCCTGAC-3’
BamE 27	5'-CACTCTGGAGCGAGTGKGCTACCGTCCTGACATC-3’
BamE 28	5'-CTGGAGCGAGTGGTTKGCCGTCCTGACATCAAC-3’
BamE 29	5'-GAGCGAGTGGTTTACKGCCCTGACATCAACCAG-3’
BamE 30	5'-GCGAGTGGTTTACCGTKGCGACATCAACCAGGGG-3’
BamE 31	5'-GTGGTTTACCGTCCTKGCATCAACCAGGGGAAC-3’
BamE 32	5'-GGTTTACCGTCCTGACKGCAACCAGGGGAACTATC-3’
BamE 33	5'-GGTTTACCGTCCTGACATCKGCCAGGGGAACTATCTG-3’
BamE 34	5'-CGTCCTGACATCAACKGCGGGAACTATCTGACC-3’
BamE 35	5’-CCTGACATCAACCAGTGCAACTATCTGACCGCTAAC-3'
BamE 36	5’-GACATCAACCAGGGGKGCTATCTGACCGCTAACG-3’
BamE 37	5’-CATCAACCAGGGGAACKGCCTGACCGCTAACGAC-3’
BamE 38	5’-CAACCAGGGGAACTATKGCACCGCTAACGACGTATC -3’
BamE 39	5’-CAGGGGAACTATCTGKGCGCTAACGACGTATCC-3’
BamE 40	5’-GGGGAACTATCTGACCKGCAACGACGTATCCAAAATAC-3’
BamE 41	5’-GAACTATCTGACCGCTKGCGACGTATCCAAAATAC-3’
BamE 42	5’-CTATCTGACCGCTAACKGCGTATCCAAAATACGTG-3’
BamE 43	5’-CTGACCGCTAACGACKGCTCCAAAATACGTGTTG-3’
BamE 44	5’-CCGCGTACGCAACTTGTTGTTGCGTCATGCCAACACGTATTTTGCMTAC GTCGTTAGCGGTC-3'
BamE 45	5’-CCGCGTACGCAACTTGTTGTTGCGTCATGCCAACACGTATGCMGGATACGTCGTTAGC -3'

BamE 46	5’-CCGCGTACGCAACTTGTTGTTGCGTCATGCCAACACGGCMTTTGGATA CGTCGTTAGC-3’
BamE 47	5’-CCGCGTACGCAACTTGTTGTTGCGTCATGCCAACGCMTATTTTGGATACGTC-3’
BamE 48	CCGCGTACGCAACTTGTTGTTGCGTCATGCCGCMACGTATTTTGGATAC-3’
BamE 49	5’-CCGCGTACGCAACTTGTTGTTGCGTCATGCAAACACGTATTTTGG-3’
BamE 50	5’-CCGCGTACGCAACTTGTTGTTGCGTGCMGCCAACACGTATTTTG-3’
BamE 51	5’-CCGCGTACGCAACTTGTTGTTGGCMCATGCCAACACGTATTTTG-3’
BamE 52	5’-CCGCGTACGCAACTTGTTGGCMCGTCATGCCAACACG-3’
BamE 53	5’-CCGCGTACGCAACTTGGCMTTGCGTCATGCCAAC-3’
BamE 54	5’-CCGCGTACGCAACGCMTTGTTGCGTCATGCCAAC-3’
BamE 55	5’-CCGCGTACGCGCMTTGTTGTT-3’
BamE 56	5’-GACGCAACAACAAGTTKGCTACGCATTGGGTACACC-3’
BamE 57	5’-GACGCAACAACAAGTTGCGKGCGCATTGGGTACACCG-3’
BamE 58	5’-GACGCAACAACAAGTTGCGTACKGCTTGGGTACACCGCTG-3’
BamE 59	5’-CCGCGTACGCAKGCGGTACAC -3’
BamE 60	5’-CCGCGTACGCATTGTGCACAC -3’
BamE 61	5’-CCGCGTACGCATTGGGTKGCCCGCTGATGTCCG-3’
BamE 62	5’-CCGCGTACGCATTGGGTACAKGCCTGATGTCCGATCC-3’
BamE 63	5’-CCGCGTACGCATTGGGTACACCGKGCATGTCCGATCCATTTGG-3’
BamE 64	5’-CCGCGTACGCATTGGGTACACCGCTGKGCTCCGATCCATTTGG-3’
BamE 65	5’-CCGCGTACGCATTGGGTACACCGCTGATGKGC -3’
BamE 66	5’-CCGCGTACGCATTGGGTACACCGCTGATGTCCKGCCCATTTGGTACGAATACC -3’
BamE 67	5’-CCGCGTACGCATTGGGTACACCGCTGATGTCCGATKGCTTTGGTACGAATACC-3’
BamE 68	5’-CCGCGTACGCATTGGGTACACCGCTGATGTCCGATCCAKGCGGTACGAATACCTGG-3’
BamE 69	5’-CCGCGTACGCATTGGGTACACCGCTGATGTCCGATCCATTTTGCACGAATACCTGGTTC-3’
BamE 70	5’-GTCCGATCCATTTGGTKGCAATACCTGGTTCTATG-3’
BamE 71	5’-CCGATCCATTTGGTACGKGCACCTGGTTCTATGTC-3’
BamE 72	5’-CCATTTGGTACGAATKGCTGGTTCTATGTCTTC-3’
BamE 73	5’-CCATTTGGTACGAATACCKGCTTCTATGTCTTCCGC-3’
BamE 74	5’-GGTACGAATACCTGGKGCTATGTCTTCCGCCAG-3’
BamE 75	5’-CGAATACCTGGTTCKGCGTCTTCCGCCAGCAAC-3’
BamE 76	5’-CGAATACCTGGTTCTATKGCTTCCGCCAGCAACC-3’
BamE 77	5’-GAATACCTGGTTCTATGTCKGCCGCCAGCAACCAGG-3’
BamE 78	5’-GGTTCTATGTCTTCKGCCAGCAACCAGGTC-3’
BamE 79	5’-GGTTCTATGTCTTCCGCKGCCAACCAGGTCATGAAG-3’
BamE 80	5’-CTATGTCTTCCGCCAGKGCCCAGGTCATGAAGGTG-3’

BamE 81	5’-GTCTTCCGCCAGCAAKGCGGTCATGAAGGTGTAAC-3’
BamE 82	5’-CTTCCGCCAGCAACCATGCCATGAAGGTGTAACTC-3’
BamE 83	5’-CCGCCAGCAACCAGGTKGCGAAGGTGTAACTCAG-3’
BamE 84	5’-CAGCAACCAGGTCATKGCGGTGTAACTCAGCAAAC-3’
BamE 85	5’-CAACCAGGTCATGAATGCGTAACTCAGCAAACG-3’
BamE 86	5’-CCAGGTCATGAAGGTKGCACTCAGCAAACGCTG-3’
BamE 87	5’-CAGGTCATGAAGGTGTAKGCCAGCAAACGCTGACG-3’
BamE 88	5’-GTCATGAAGGTGTAACTKGCCAAACGCTGACGCTG-3’
BamE 89	5’-GAAGGTGTAACTCAGKGCACGCTGACGCTGACC-3’
BamE 90	5’-GGTGTAACTCAGCAAKGCCTGACGCTGACCTTTAAC-3’
BamE 91	5’-GTAACTCAGCAAACGKGCACGCTGACCTTTAAC-3’
BamE 92	5’-GTAACTCAGCAAACGCTGKGCCTGACCTTTAACAGTAG-3’
BamE 93	5’-CAGCAAACGCTGACGKGCACCTTTAACAGTAGC-3’
BamE 94	5’-CAAACGCTGACGCTGKGCTTTAACAGTAGCGGTG-3’
BamE 95	5’-CAAACGCTGACGCTGACCKGCAACAGTAGCGGTGTG-3’
BamE 96	5’-CTGACGCTGACCTTTKGCAGTAGCGGTGTGTTG-3’
BamE 97	5’-GACGCTGACCTTTAACKGCAGCGGTGTGTTGACC-3’
BamE 98	5’-CTGACCTTTAACAGTKGCGGTGTGTTGACCAATATTG-3’
BamE 99	5’-GACCTTTAACAGTAGCTGCGTGTTGACCAATATTG-3’
BamE 100	5’-CTTTAACAGTAGCGGTKGCTTGACCAATATTGATAAC-3’
BamE 101	5’-CTTTAACAGTAGCGGTGTGKGCACCAATATTGATAAC-3’
BamE 102	5’-CAGTAGCGGTGTGTTGKGCAATATTGATAACAAAC-3’
BamE 103	5’-CCGGAATTCTTAGTTACCACTCAGCGCAGGTTTGTTATCAATGCMGGTCAACACACCGCTAC-3’
BamE 104	5’-CCGGAATTCTTAGTTACCACTCAGCGCAGGTTTGTTATCGCMATTGGTCAACACACC-3’
BamE 105	5’-CCGGAATTCTTAGTTACCACTCAGCGCAGGTTTGTTGCMAATATTGGTCAACAC-3’
BamE 106	5’-CCGGAATTCTTAGTTACCACTCAGCGCAGGTTTGCMATCAATATTGGTCAAC-3’
BamE 107	5’-CCGGAATTCTTAGTTACCACTCAGCGCAGGGCMGTTATCAATATTGGTC-3’
BamE 108	5’-CCGGAATTCTTAGTTACCACTCAGCGCGCMTTTGTTATCAATATTG-3’
BamE 109	5’-CCGGAATTCTTAGTTACCACTCAGGCMAGGTTTGTTATCAATATTG-3’
BamE 110	5’-CCGGAATTCTTAGTTACCACTGCMCGCAGGTTTGTTATC-3’
BamE 111	5’-CCGGAATTCTTAGTTACCGCMCAGCG-3’
BamE 112	5’-CCGGAATTCTTAGTTGCAACTCAGCGC-3’
BamE 113	5’-CCGGAATTCTTAGCMAACACTCAGCG-3’

SUPPLEMENTARY METHODS

Complementation assays. Competent cells, containing the *bamE::Kan* mutation from the Keio collection (Baba et al, 2006), were transformed with pBAME derivatives from the BamE mutant library. Bacterial cultures were grown overnight in LB medium supplemented with 100 µg/ml ampicillin, diluted 1 in 100 and printed onto LB agar plates supplemented with 100 µg/ml ampicillin and vancomycin ranging from 0 to 110 µg/ml. Complementation was assessed by monitoring growth on the vancomycin plates in comparison to *bamE::Kan* cells carrying either pBAME derivatives or pET20b empty vector.

Western blotting. Cells cultures of the *bamE::Kan* mutant strain carrying pET20b, pBAME derivatives from the BamE glycine library were grown. Total cellular protein was prepared and subjected to Western blotting as detailed previously (Desvaux et al, 2007). BamE was detected using anti-BamE antiserum raised in rabbit.

Sucrose density-gradient centrifugation. Bacterial cells (250 ml) were harvested by centrifugation (10, 000 *g*, 10 min, 4°C), washed and re-suspended in buffer M (50 mM triethanolamine [TEA], 1 mM dithiothreitol [DTT], 1 mM ethylenediaminetetraacetic acid [EDTA], pH 7.5) containing Complete protease inhibitors (Roche). The cells were lysed using a French pressure cell at 20,000 pounds per square inch and centrifuged as before to remove cell debris and unlysed cells. The supernatant was centrifuged (50, 000 *g*, 2 h, 4°C) to pellet the total cell membrane. The membrane pellet was washed in buffer M, and centrifuged again. The final membranes were homogenized in 3.5 ml buffer M and transferred on top of a five-step sucrose gradient to separate the inner and outer membrane fractions. Sucrose gradients were prepared in buffer M by layering sucrose solutions into 14 x 95 mm ultracentrifuge tubes (Beckman) as follows (from bottom to top): 0.8 ml at 55%, 3.0 ml at 50%, 3.0 ml at 47%, 2.0 ml at 42% and 0.8 ml at 30% (all w/w). Sucrose gradients were centrifuged (210,000 *g*, 16 h, 4°C) in an SW 40 Ti rotor (Beckman), and 500 µl fractions were collected through

gravity flow after puncturing the bottom of each gradient with a needle. Outer membrane fractions were pooled and dialyzed against Milli-Q water to remove the sucrose.

Mass spectrometry and statistical analysis. Metabolites were extracted using a two-step methanol:water:chloroform protocol (Wu et al, 2008). The nonpolar extracts were dried under nitrogen and then taken up in their original volume (220-550 µl) of chloroform:methanol (1:3). These were then stored at -80°C until analysis. A quality control sample was pooled from 50-µl aliquots of six representative samples. Immediately prior to analysis, samples were diluted 5-fold in chloroform:methanol (1:3) for mass spectrometric analysis in both the positive and negative ion modes. Fourier transform ion cyclotron resonance (FT-ICR) mass spectrometry was performed using a LTQ FT Ultra instrument (Thermo Scientific, Bremen, Germany) equipped with a chip-based direct infusion nanoelectrospray ion source (Triversa, Advion Biosciences, Ithaca, NY). Spectra were acquired for 0.5 min each, after a 0.5 min delay, from *m/z* 160 to 1600. The spray voltage was set to +1.5 and -1.5 kV, respectively, and samples analyzed in triplicate in a predetermined, randomized order. Data processing included application of the SIM-stitching algorithm (Southam et al, 2007), probabilistic quotient normalisation (Dieterle et al, 2006), and the generalised log transformation (Parsons et al, 2007). Principal components analysis (PCA) was initially used to assess the overall metabolic differences between the sample groups in an unbiased manner, using the PLS_Toolbox (version 5.5.1, Eigenvector Research, Manson, WA, USA) within Matlab (version 7.8; The MathsWorks, Natick, MA, USA). Individual lipids within classes of particular interest (e.g., glycerophosphoethanolamines and glycerophosphoglycerols) were identified based on accurate mass (*m/z*) measurements and fragmentation data (MS/MS by Pulsed Q Collision Induced Dissociation in the ion trap). Univariate statistical analysis were used to determine if these individual lipids changed intensities significantly, performed using

an in-house, R-based ANOVA script with a false discovery rate of 5% to correct for multiple hypothesis testing, and Excel.

SUPPLEMENTARY FIGURES

Figure S1 – BamE is monomeric in the periplasm and multimerizes in the cytoplasm. (A) Size exclusion profile of HisTrap purified BamE on a Superdex 75 10/300GL (GE Healthcare) column after extraction from the periplasm, following expression at 30^{o}C for 4 hours. (B) Size exclusion profile of HisTrap purified BamE on a Superdex 75 10/30GL (GE Healthcare) after extraction from whole cells, following expression at 30^{o}C for 4 hours. Monomer and dimer peaks are denoted by "M" and "D", respectively. (C) Superdex 75 26/60PG (GE Healthcare) size exclusion profile of HisTrap purified BamE extracted from whole cells, following expression at 20^{o}C for 4 hours. (D) Superdex 75 26/60PG (GE Healthcare) size exclusion profile of HisTrap purified BamE extracted from whole cells, following expression at 37^{o}C for 4 hours. (E) HSQC spectrum of 0.2 mM ^{15}N BamE following periplasmic purification as shown in (A), assignments are reported in (Knowles et al, 2010). (F) HSQC spectrum of 0.2 mM ^{15}N BamE following whole cell purification as shown in (B). 50 mM sodium phosphate pH 7 with 300 mM sodium chloride at 20^{o}C was used throughout. The structure of the dimeric state has not been determined due to its absence from the native environment of the periplasm.

Figure S2 – DaliLite structure based alignment of BamE and OmlA amino acid sequences. SS-BamE and SS-OmlA refers to the secondary structural elements of BamE and OmlA (2PXG), respectively, where H, E and L correspond to helical, extended and loop sequences.

Figure S3 – Phenotype microarray data. Wild-type *E. coli* BW25113 and an isogenic *bamE* mutant were analysed using Phenotype Microarrays (BioLog^{TM}) for chemical sensitivity for bacteria (PM plates 11-20). Arrays were conducted in triplicate over a 24 hour period. Data shown depicts the respiration rates of bacteria derived from one replicate. Green

curves represent data derived for wild-type bacteria; red curves represent data derived for mutant bacteria. Where the respiration rates of both wild-type and mutant are similar they appear as yellow curves. The drug content of each well can be found at www.biolog.com/pdf/PM11-PM20.pdf. The position of vancomycin in the assay is depicted. Both mutant and wild-type can survive equally well at lower concentrations of vancomycin but at higher concentrations the mutant fails to grow. Marginal defects in growth were observed for several other antibiotics. All conditions showing differences in growth in the Biolog assay were tested manually under standard laboratory conditions. Vancomycin reproducibly inhibited growth of Δ*bamE* strains. The Δ*bamE* mutant did not outperform the WT under any condition.

Figure S4 –Vancomycin sensitivity of *bamE* cells containing plasmids from the BamE mutant library. The panels show the concentration of vancomycin necessary to prevent growth of *ΔbamE E. coli* cells expressing pET20b plasmids encoding BamE mutants bearing either (A) glycine or (B) cystene substitutions, on Luria Broth agar plates supplemented with 100ug/ml ampicillin. Each value is the median concentration of vancomycin obtained from at least three independent experiments.

Figure S5 – Western blot analysis of BamE expression levels. Western blot analysis showing total cellular BamE expression of a representative selection of BamE mutants. The lanes correspond to cells which are (1) devoid of BamE, (2) express wild-type BamE, or (3-20) representative selection of mutant BamE forms from a *bamE* mutant strain containing pET20b, pBAME or pBAME derivative from the BamE glycine mutation library, respectively, as probed with anti-BamE antiserum.

Figure S6 – BamE Sequence alignment. The sequence of *E.coli* BamE is shown first, followed by homologues listed by their Genbank Accession numbers. Asterisks represent residues shown to be functionally important. The alignment is representative of >350 BamE alleles derived from all the Gram-negative bacteria whose genomes have been sequenced.

Figure S7 - BamE does not bind DHPE nor cardiolipin. - (A) Histogram showing the normalised chemical shift perturbations induced in ^{15}N BamE (100 μM) on addition of di-hexanoyl phosphatidylethanolamine (DHPE) (40 mM). (B) Histogram showing the normalised chemical shift perturbations induced in ^{15}N BamE (100 μM) on addition of DHPE/cardiolipin (24 mM/2.4 mM), with DHPE being used to solubilise cardiolipin. Normalised chemical shifts calculated according to the equation $\Delta\delta_{ave} = \sqrt{(\Delta\delta_{HN} \times 500)^2 + (\Delta\delta_N \times 50.7)^2}$ where $\Delta\delta_{HN}$ and $\Delta\delta_N$ are the chemical shifts for amide proton and ^{15}N signals, respectively (C) Chemical shift perturbations shown for T70 and N71 on addition of DHPG. Larger changes in chemical shift were noted in BamE resonances between 20 and 30 mM DHPG, just above the critical micellar concentration of DHPG which is approximately 20 mM (Tan & Roberts, 1996).

Figure S8 – BamE(F74A) is folded. The lineshapes and dispersion of peaks shown in the superimposed HSQC spectra of the WT (Red) and F74A (Blue) mutant BamE proteins, which are both ^{15}N labelled, are substantially similar, indicating that both are folded.

Figure S9 – Formation of a ternary complex of BamE, BamD and DHPG (A) $^{1}H^{15}N$-HSQC-monitored titration of a complex of 300 µM ^{15}N-BamE/BamD (Black spectrum) with 20mM DHPG (Red spectrum). Selected chemical shift perturbations are shown by arrows and show interaction of BamE with DHPG whilst still bound to BamD. Chemical shift perturbations occur for all residues previously found to interact with BamD, Although the positions of shifted peaks are altered due to the additional presence of DHPG in the complex. (B) $^{1}H^{15}N$-HSQC monitored titration of a complex of 300 µM ^{15}N-BamE and 25mM DHPG (Blue) with 500 µM BamD (Red). The loss of peak intensity is due to line broadening and is indicative of formation of a large, slowly tumbling complex of BamD upon binding to BamE. The lack of chemical shift changes back to those of the binary BamE/BamD complex state but to those of the ternary complex observable in (A) indicates that DHPG remains bound to BamE upon its interaction with BamD.

Figure S10 – Changes in abundance of the total classes of PE and PG lipids. Shown are the overall levels of PE and PG lipids in wild type (WT) versus *ΔbamE* independent Keio library knockouts (M1 and M2). Results show the mean ± one standard deviation based on triplicate experiments. The BamE deletions do not cause any change in the abundance of the PG lipids relative to the wild type.

Supplementary Figure 1 - Knowles et al.

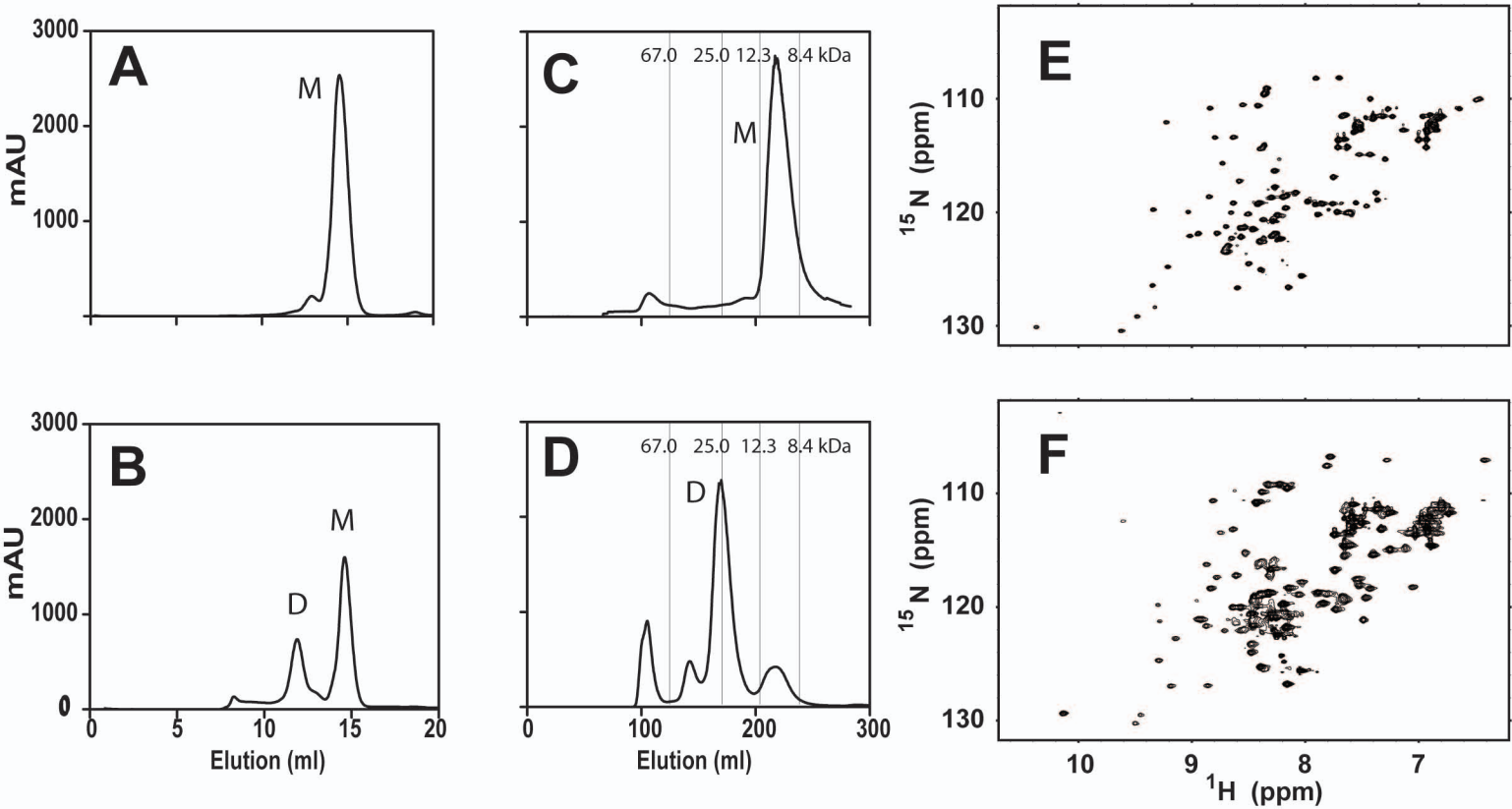

Supplementary Figure 2 – Knowles et al.

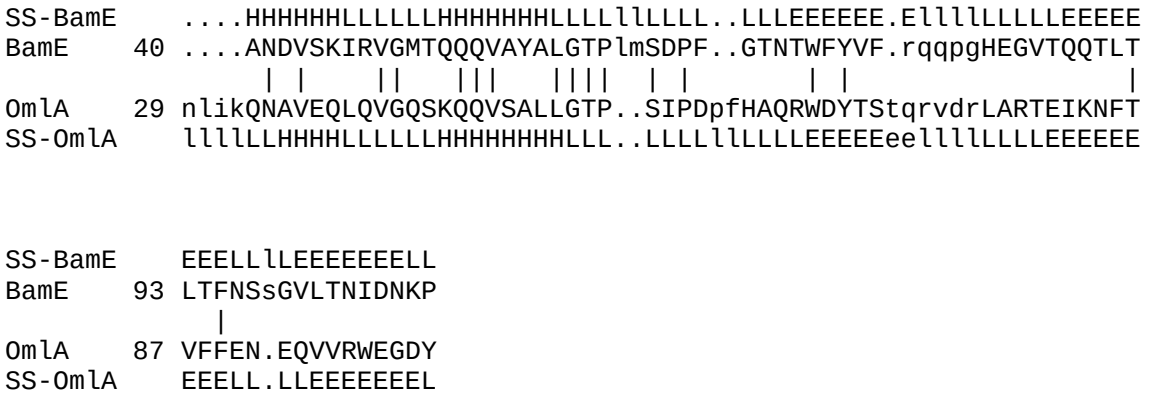

Supplementary Figure 3 - Knowles et al.

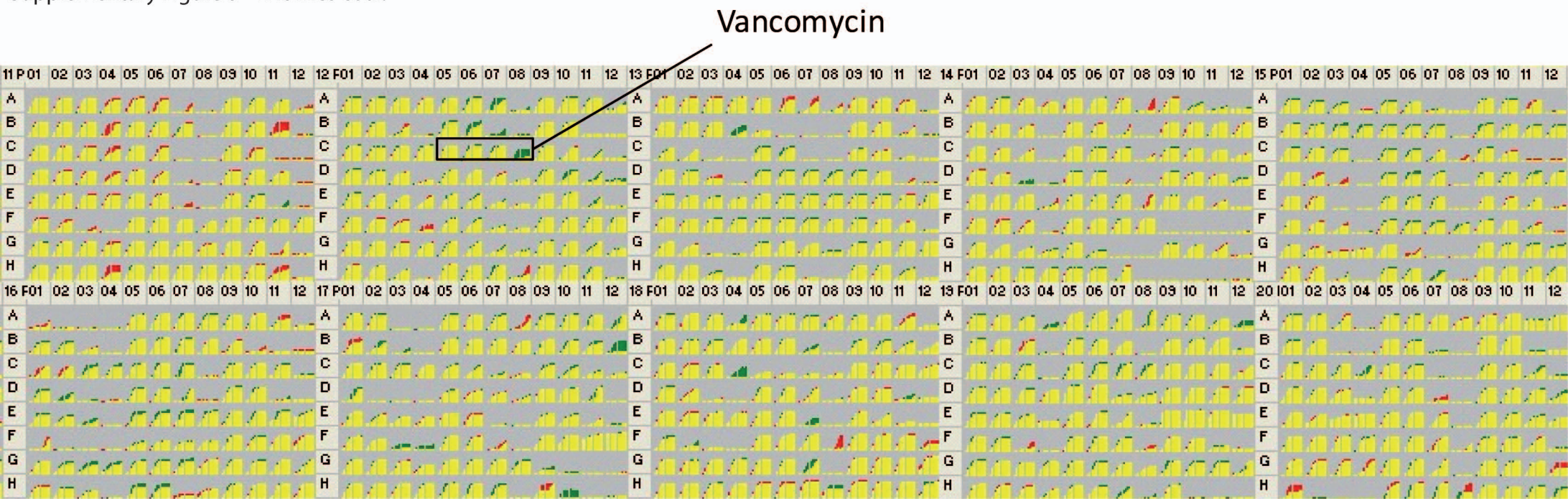

Supplementary Figure 4 – Knowles et al.

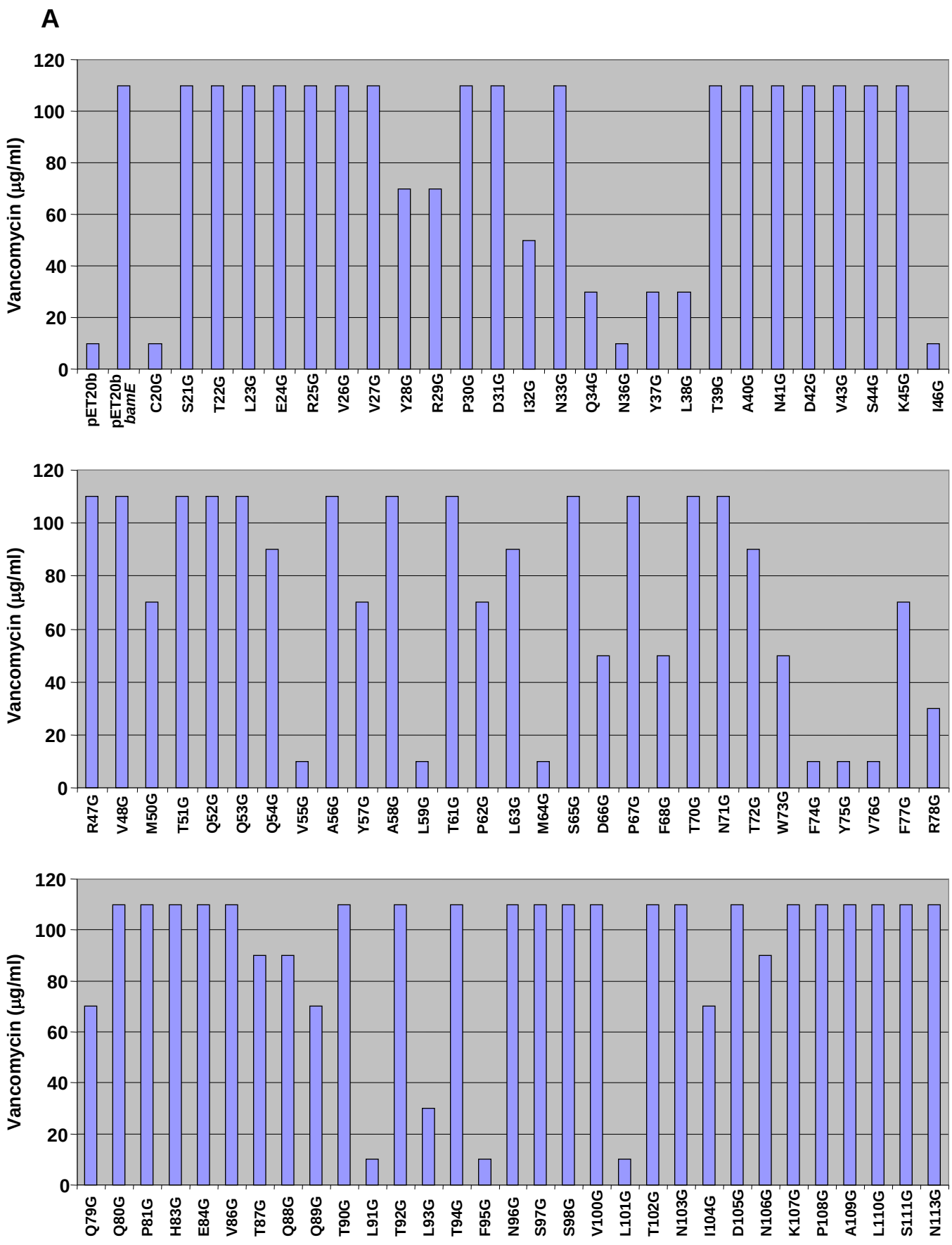

B

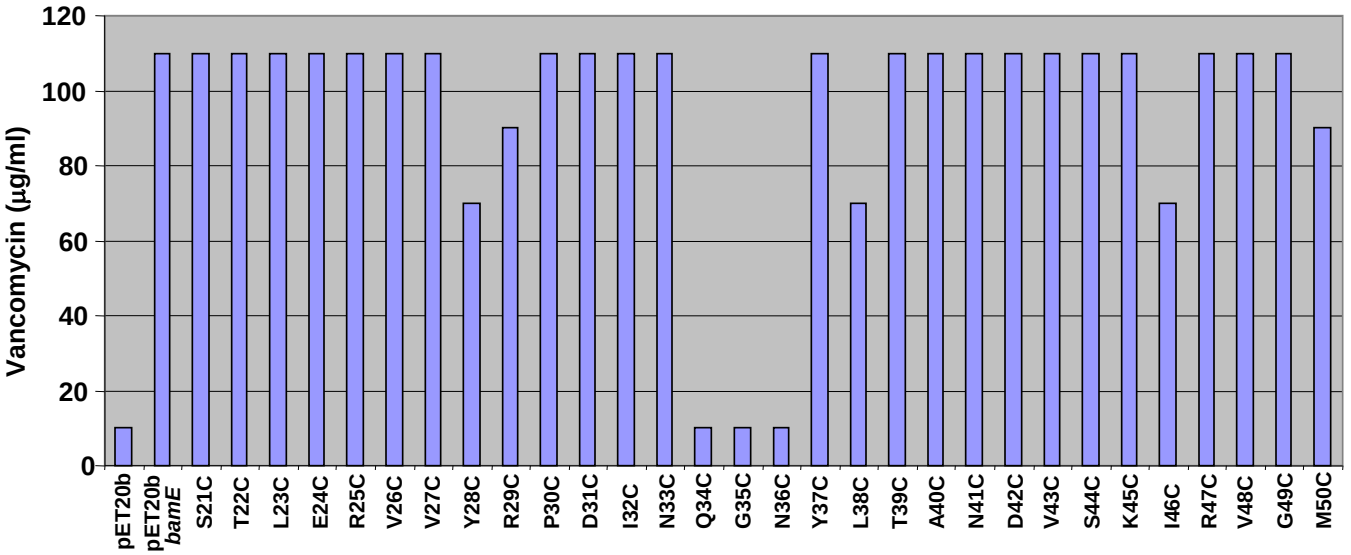
Vancomycin (µg/ml)
0
20
40
60
80
100
120
pET20b
pET20b bamE
S21C
T22C
L23C
E24C
R25C
V26C
V27C
Y28C
R29C
P30C
D31C
I32C
N33C
Q34C
G35C
N36C
Y37C
L38C
T39C
A40C
N41C
D42C
V43C
S44C
K45C
I46C
R47C
V48C
G49C
M50C

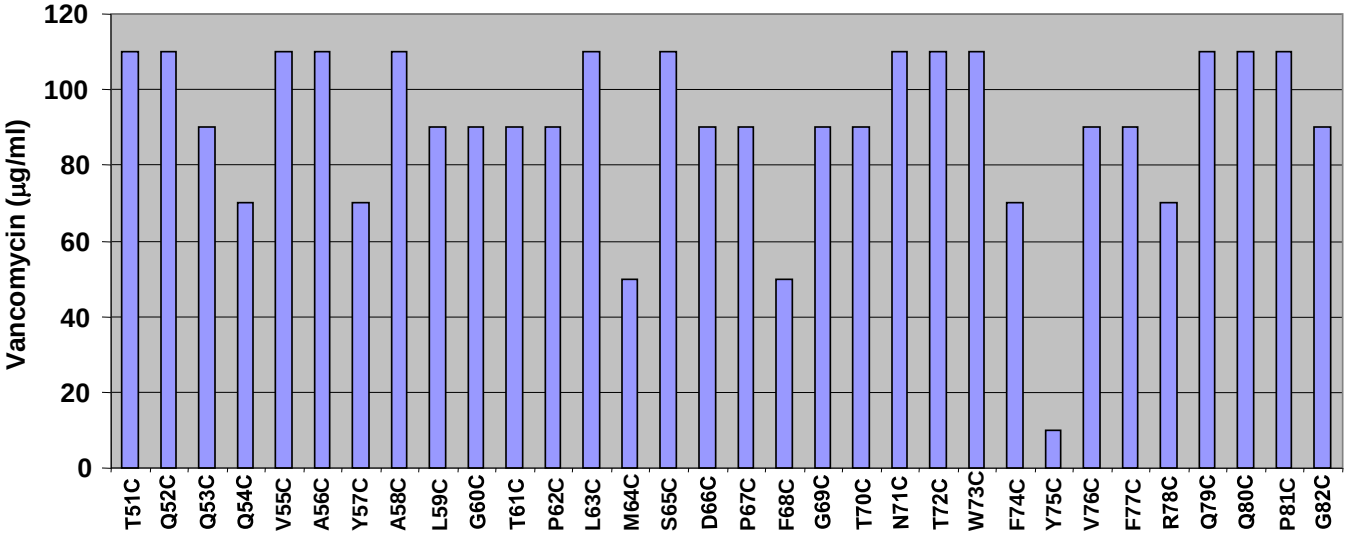
Vancomycin (µg/ml)
0
20
40
60
80
100
120
T51C
Q52C
Q53C
Q54C
V55C
A56C
Y57C
A58C
L59C
G60C
T61C
P62C
L63C
M64C
S65C
D66C
P67C
F68C
G69C
T70C
N71C
T72C
W73C
F74C
Y75C
V76C
F77C
R78C
Q79C
Q80C
P81C
G82C

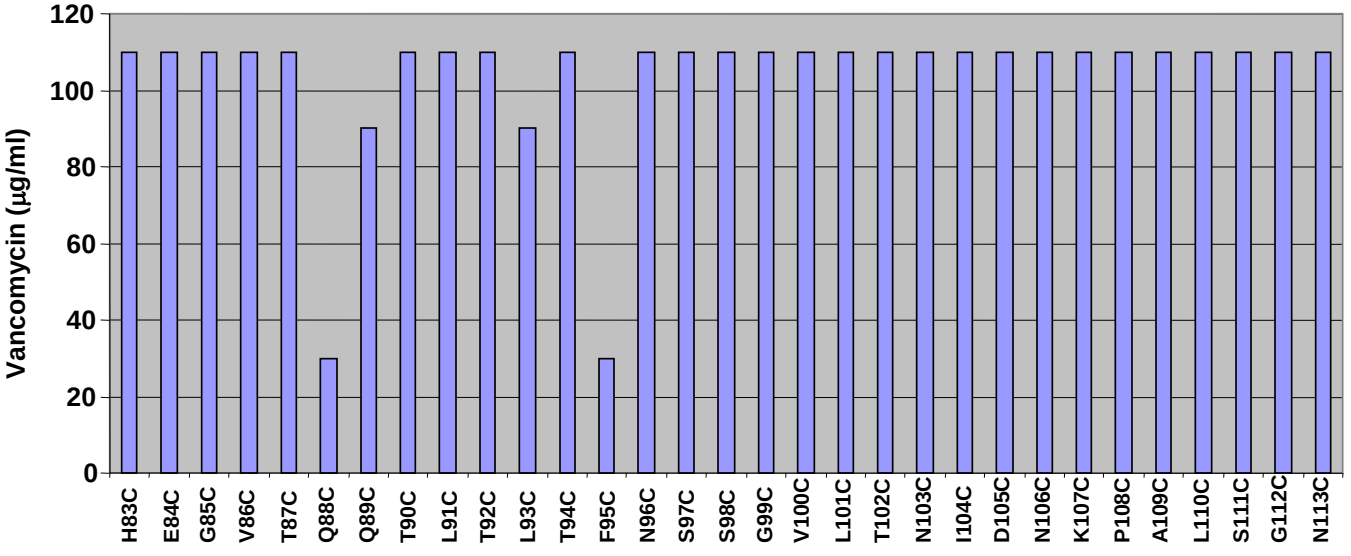
Vancomycin (µg/ml)
0
20
40
60
80
100
120
H83C
E84C
G85C
V86C
T87C
Q88C
Q89C
T90C
L91C
T92C
L93C
T94C
F95C
N96C
S97C
S98C
G99C
V100C
L101C
T102C
N103C
I104C
D105C
N106C
K107C
P108C
A109C
L110C
S111C
G112C
N113C

Supplementary Figure 5 – Knowles et al.

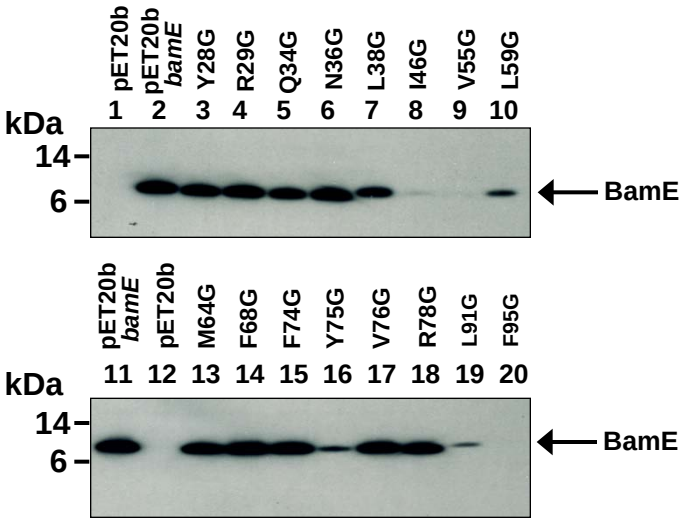

Supplementary Figure 6 – Knowles et al.

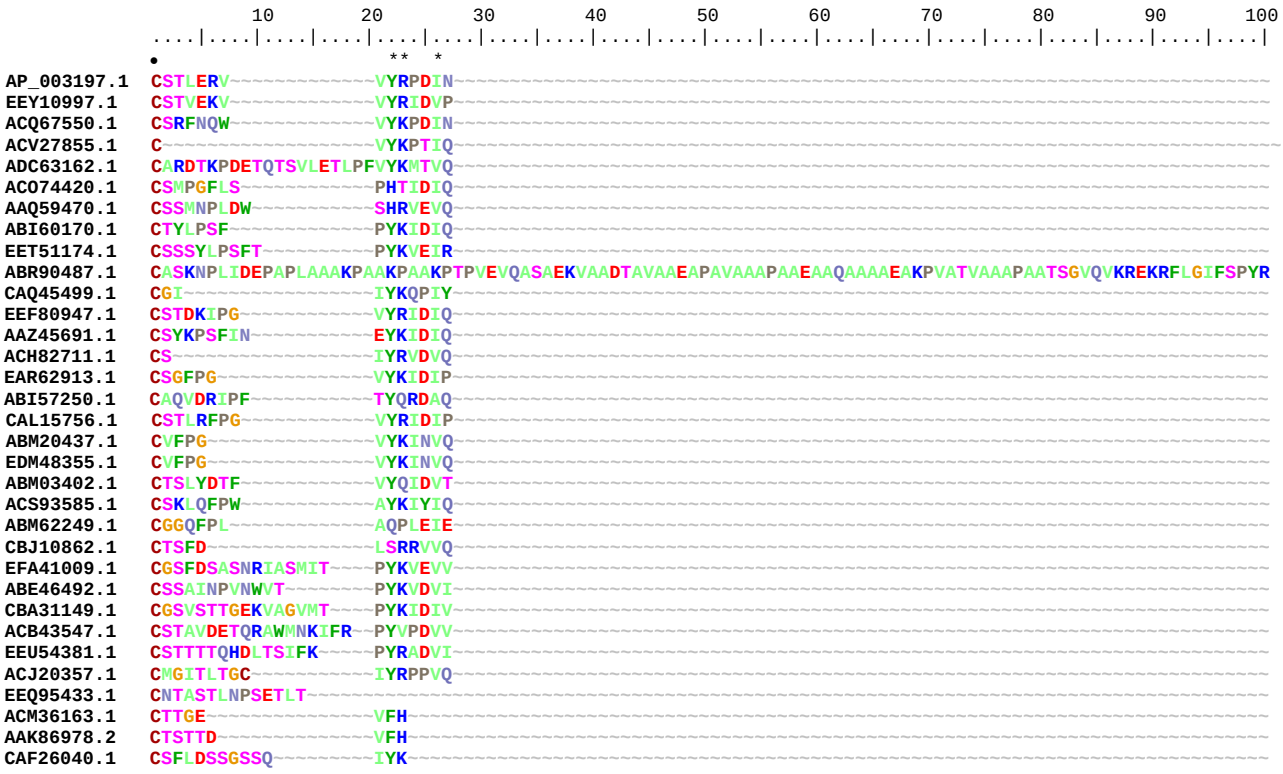

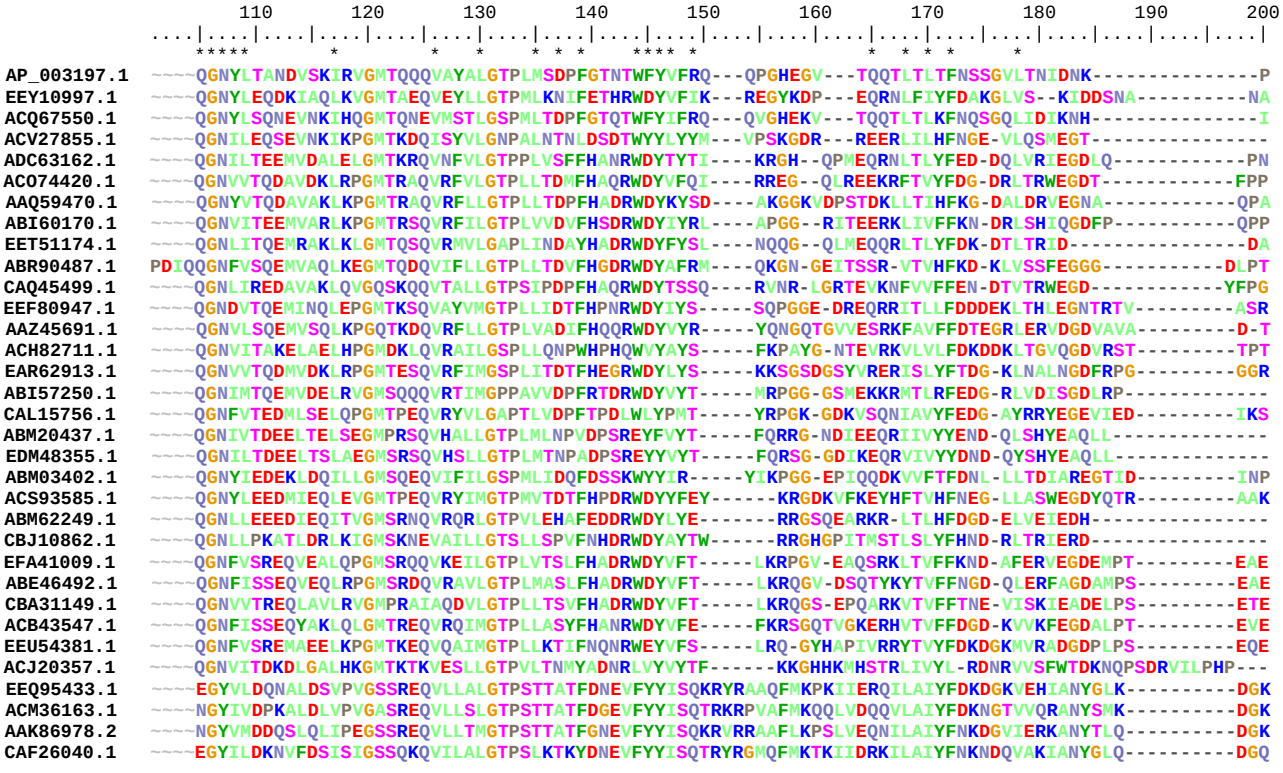

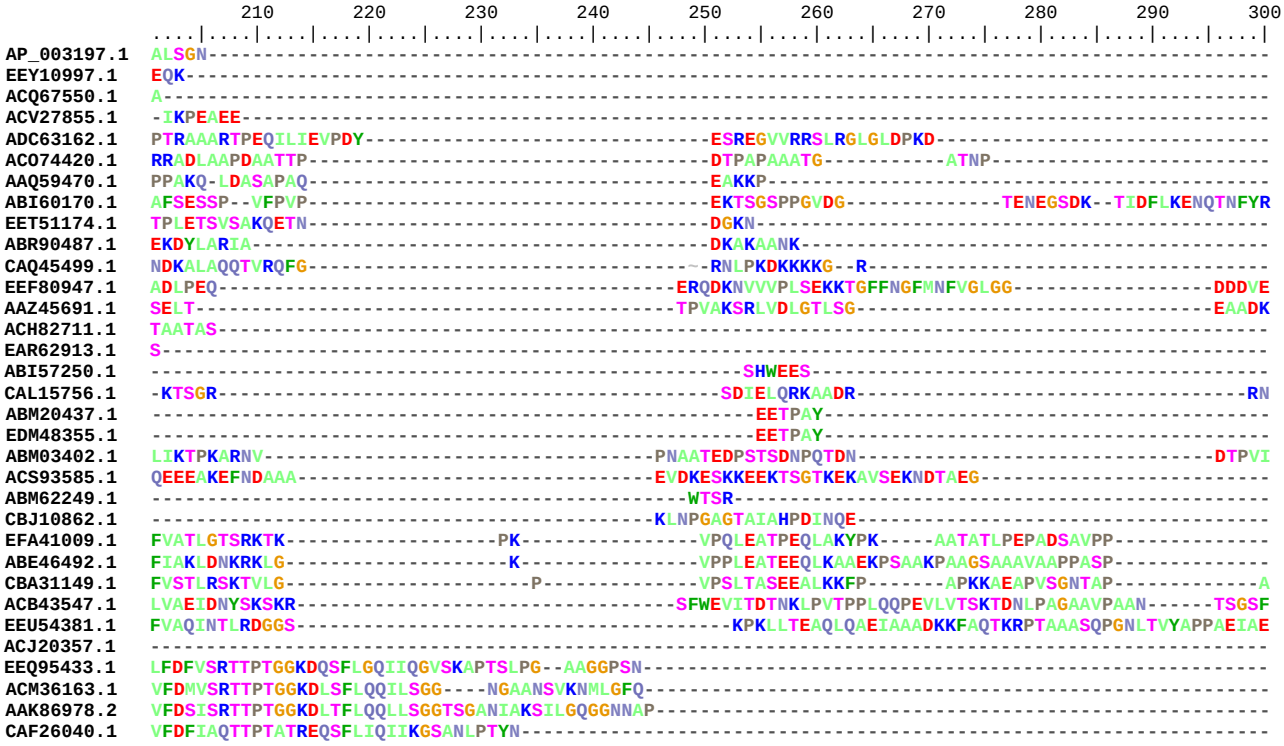
210 220 230 240 250 260 270 280 290 300
AP_003197.1
EEY10997.1
ACQ67550.1
ACV27855.1
ADC63162.1
ACO74420.1
AAQ59470.1
ABI60170.1
EET51174.1
ABR90487.1
CAQ45499.1
EEF80947.1
AAZ45691.1
ACH82711.1
EAR62913.1
ABI57250.1
CAL15756.1
ABM20437.1
EDM48355.1
ABM03402.1
ACS93585.1
ABM62249.1
CBJ10862.1
EFA41009.1
ABE46492.1
CBA31149.1
ACB43547.1
EEU54381.1
ACJ20357.1
EEQ95433.1
ACM36163.1
AAK86978.2
CAF26040.1

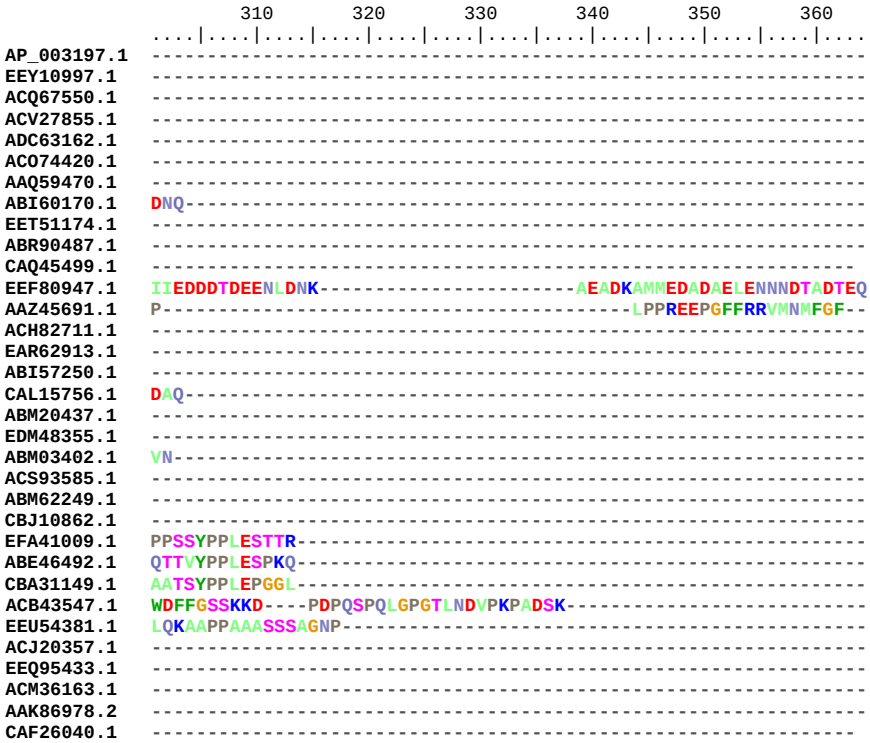
310 320 330 340 350 360
AP_003197.1
EEY10997.1
ACQ67550.1
ACV27855.1
ADC63162.1
ACO74420.1
AAQ59470.1
ABI60170.1
EET51174.1
ABR90487.1
CAQ45499.1
EEF80947.1
AAZ45691.1
ACH82711.1
EAR62913.1
ABI57250.1
CAL15756.1
ABM20437.1
EDM48355.1
ABM03402.1
ACS93585.1
ABM62249.1
CBJ10862.1
EFA41009.1
ABE46492.1
CBA31149.1
ACB43547.1
EEU54381.1
ACJ20357.1
EEQ95433.1
ACM36163.1
AAK86978.2
CAF26040.1

Supplementary Figure 7 - Knowles et al.

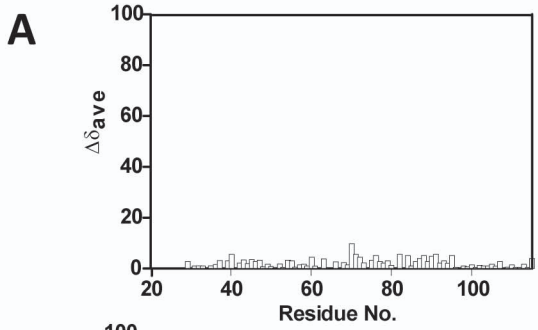

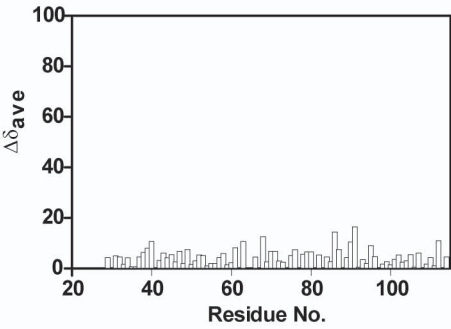

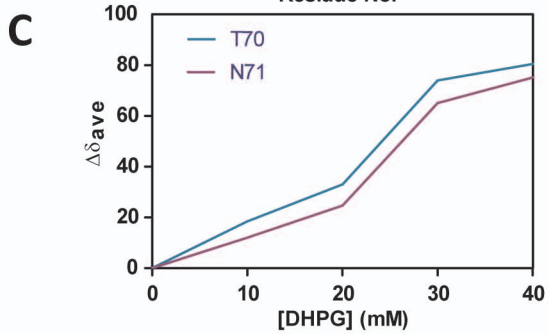

Supplementary Figure 8 - Knowles et al.

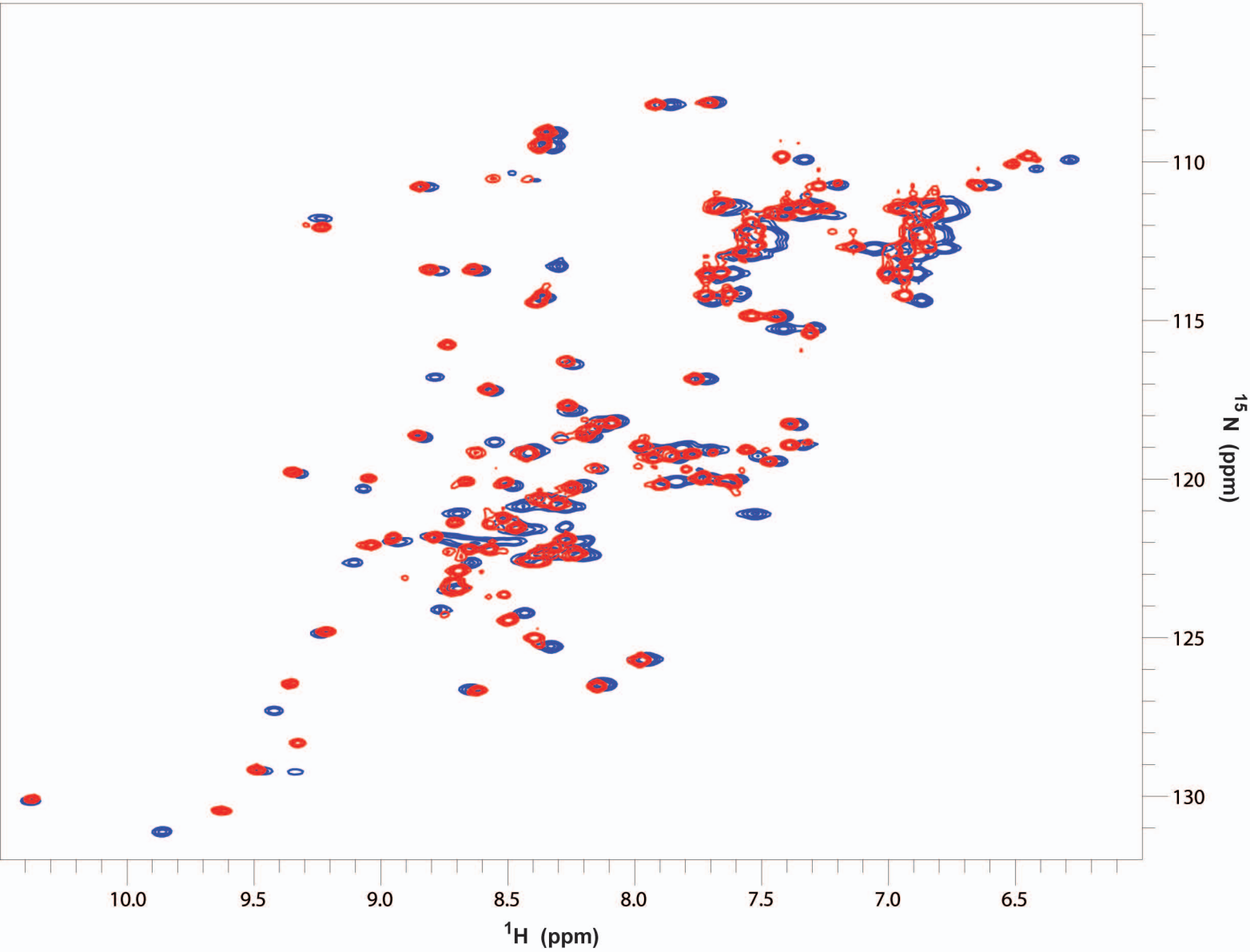

Supplementary Figure 9 - Knowles et al.

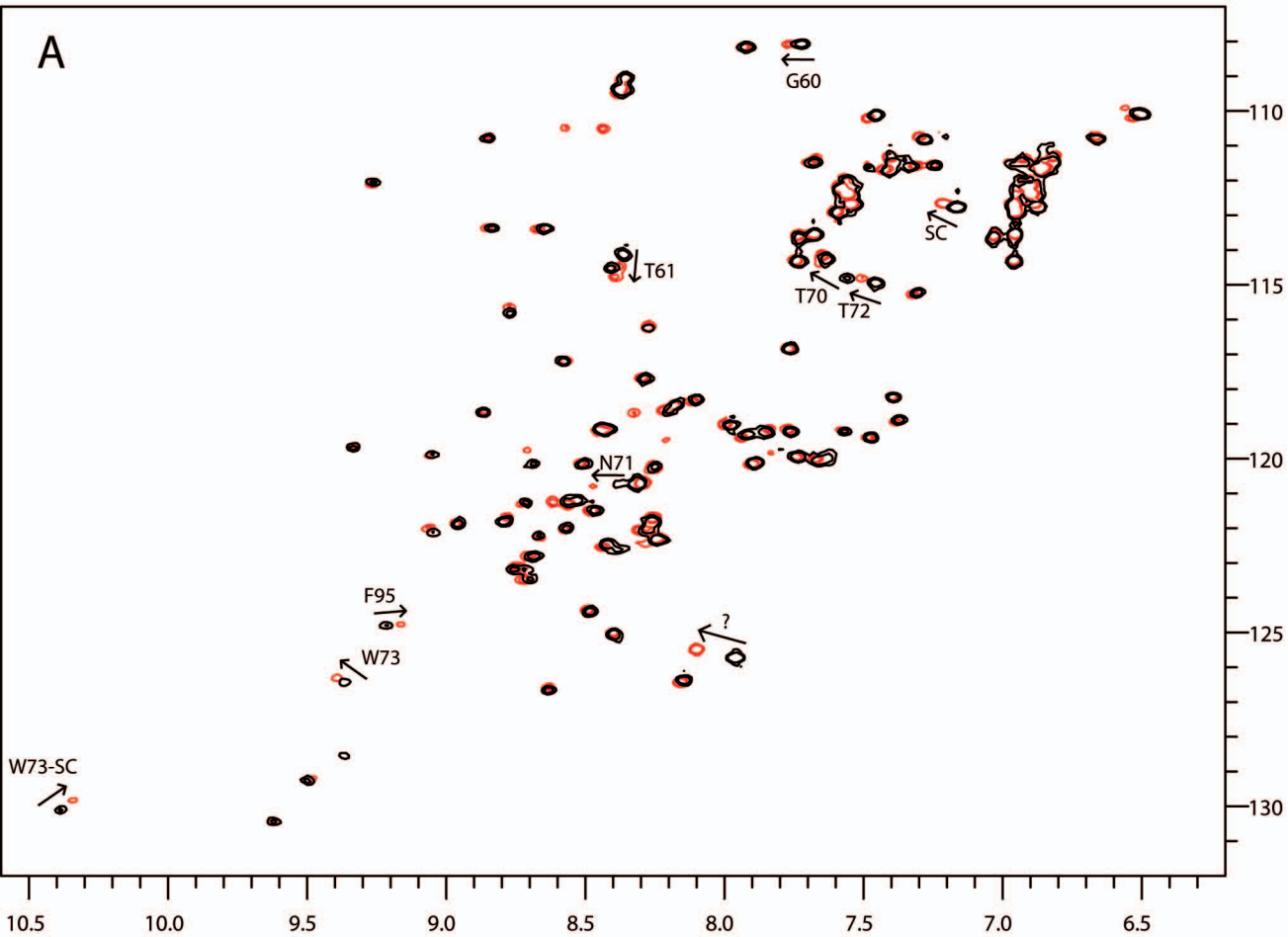

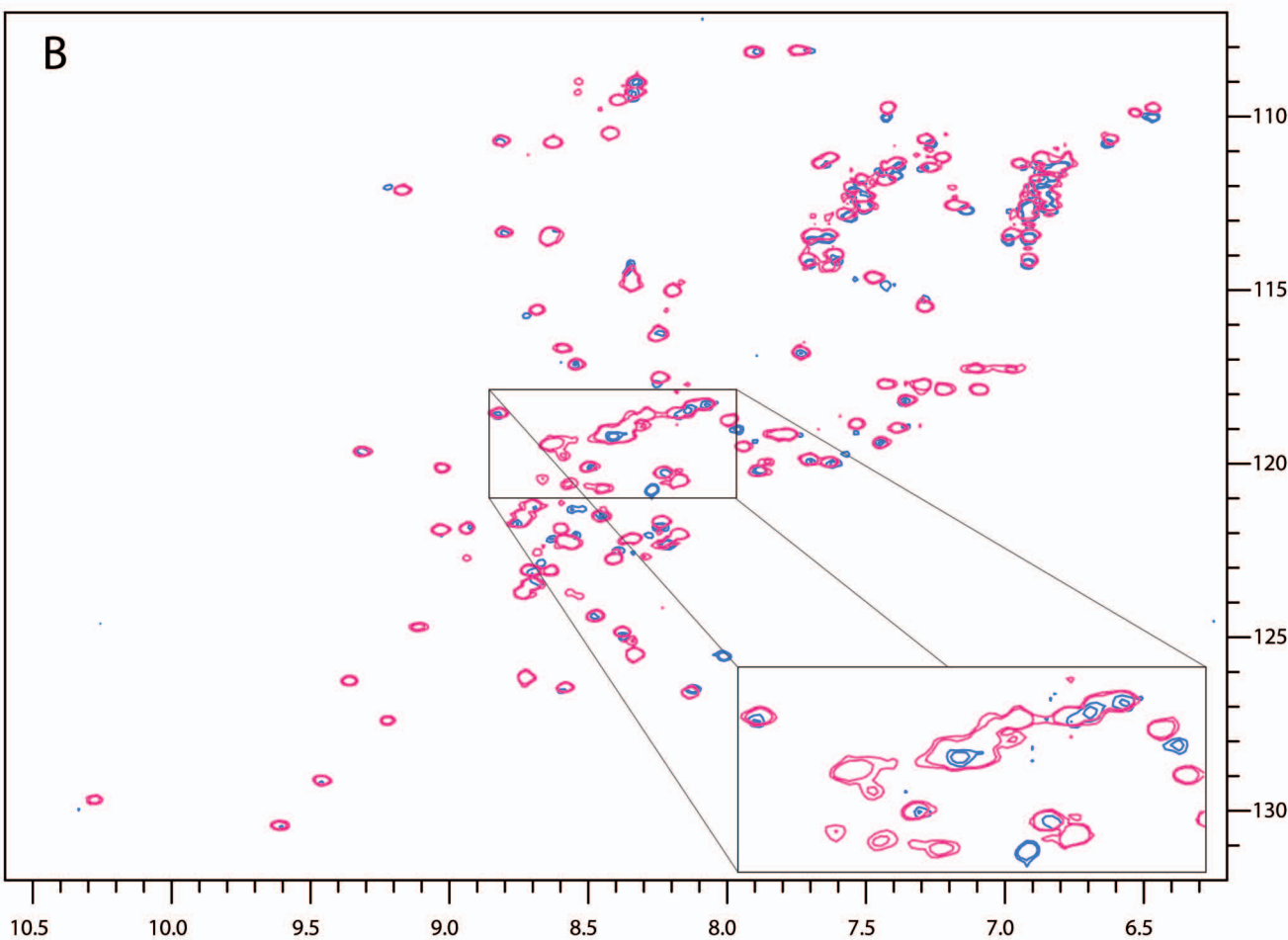

Supplementary Figure 10 - Knowles et al.